Vietnam Journal of Earth Sciences, 45(1), 1-18, https://doi.org/10.15625/2615-9783/17490

Vietnam Journal of Earth Sciences
https://vjs.ac.vn/index.php/jse

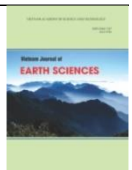

Ionospheric quasi-biennial oscillation of the TEC amplitude of the equatorial ionization anomaly crests from continuous GPS data in the Southeast Asian region

Dung Nguyen Thanh[1,2], Minh Le Huy[1,2*], Christine Amory-Mazaudier[3], Rolland Fleury[4], Susumu Saito[5], Thang Nguyen Chien[1], Thanh Le Truong[1], Hong Pham Thi Thu[1,2], Thanh Nguyen Ha[1], Mai Nguyen Thi[1], Que Le[6]

[1]*Institute of Geophysics, VAST, Hanoi, Vietnam*
[2]*Graduate University of Science and Technology, VAST, Hanoi, Vietnam*
[3]*Sorbonne Université, UPMC Univ. Paris 06, Paris, France*
[4]*LAB-STICC, UMR 6285, Institut Mines-Telecom Atlantique, France*
[5]*Electronic Navigation Research Institute, MPAT, Japan*
[6]*International University, Vietnam National University, Ho Chi Minh City, Vietnam*

Received 02 June 2022; Received in revised form 19 August 2022; Accepted 01 September 2022

ABSTRACT

The quasi-biennial oscillation (QBO) signals at two Equatorial ionization anomaly (EIA) crests of the ionosphere have been studied using the continuous GNSS network data in Vietnam and adjacent regions during the 2008- 2021 period. The monthly mean EIA crests amplitudes are calculated. The Lomb-Scargle periodogram method was applied to the residuals of the EIA crests magnitudes, ΔTEC, which are obtained from subtracting the fittings with solar index, F10.7. The Lomb-Scargle spectrum shows the quasi-biennial component in the residuals ΔTEC with the picks at 18, 25, and 29-30 months. The ionosphere QBO at two EIA crests was found out by the band-pass filter centered at 25 months with haft-power points at 17 and 33 months. The zonal wind data at 50 hPa (~20 km) of the tropical equatorial stratosphere is used as the stratosphere QBO (SQBO) to consider the relationship between the SQBO and the obtained ionosphere QBO. The direct comparison and the cross wavelet transform of the SQBO and ionosphere QBO data series show that during 2008-2009, the ionosphere QBO signal is low, the SQBO and ionosphere QBO are in phase during the 2010-2013 and 2018-2021 periods, but anti-phase during the 2014-2017 period. For the 2010-2013, 2014-2017 and 2018-2021 periods, the correlation coefficients are 0.623, -0.646, 0.637 in the northern crest, and 0.571, -0.530, 0.530 in the southern crest, respectively. Furthermore, we also observed that the SQBO and the ionosphere QBO signals were shortened during the 2015-2016 period, approximately 1.5 years. Previous studies showed that the ENSO (El Niño - Southern Oscillation) warm phase, also known as El-Niño existed during 2015-2016. The results of this study allow us to assume that the SQBO influences the ionosphere QBO. Our results show that the SQBO is the main factor affecting the ionospheric QBO at two EIA crests. However, the physical theoretical interpretation of the mechanisms of action is a challenge for scientists and requires further research.

Keywords: Equatorial Ionization Anomaly, Stratosphere Quasi-Biennial Oscillations (SQBO), ionosphere QBO, GNSS, ΔTEC, Southeast Asian region.

1. Introduction

The stratosphere Quasi Biennial Oscillation (SQBO) is a variation of zonal wind of the lower stratosphere at the tropical, which was promoted by waves transmitted upward from the lower atmosphere; this means flow

*Corresponding author, Email: lhminh@igp.vast.vn

in the tropical stratosphere at the height of of about 18-50 km (~70 hPa-1 hPa). Its phase is eastward or westward of mean zonal wind at the lower stratosphere at about 30 hPa (~25 km). In the early 1960s, bands of easterly and westerly winds at the equatorial stratosphere were found to move alternately with a variable period averaging approximately 26 months (Reed et al., 1961; Ebdon and Veryard, 1961). Since then, the periods of the SQBO have been identified to range between 22 and 34 months, and the average period is approximately 28 months (Wallace & Kousky, 1968). The wind observations by electric radio wave at the tropical, which was performed continuously from 1953 and gave evidence about SQBO (e.g., Naujokat, 1986), and the initial observations are available time series for the now which was saved at the Free University of Berlin, Germany (http://www.geo.fu-berlin.de/en/met/ag/strat/product/qbo/). SQBO is important in dominating the variability of the tropical lower stratosphere meteorology (Wallace, 1973). Although SQBO is a tropical atmosphere phenomenon, it also affects the global atmospheric circulation at latitudes and altitudes outside the tropical stratosphere (Labitzke, 1987; Labitzke and van Loon, 1988; Ford et al., 2009; Murphy et al., 2012, Espy et al., 2011; Hibbins et al., 2009; Xu et al., 2009; Burrage et al., 1996; Venkat Ratnam et al., 2008). SQBO is also very important for seasonal forecasting, and it also controls the variation of ozone and stratosphere water which can modulate ultraviolet (UV) and infrared (IR) radiation on the Earth's surface. A comprehensive overview of SQBO (together with a description of the causes of SQBO) can be found in Baldwin et al. (2001). SQBO significantly modulates Planetary Waves (PWs) that travel during winter in Northern Hemisphere (NH) (Hibbins et al., 2009). Modulation was found to be stronger for waves propagating eastward and standing waves and weaker for waves propagating westward (Lu et al., 2012). Furthermore, SQBO even modulates extratropical waves and influences polar stratospheric flows. It has been found that SQBO modulates the Polar Vortex (PV) of the stratosphere in the winter in Northern Hemisphere through interactions between mean flow and wave (Yadav et al., 2019). This causes a relationship between equatorial circulation which is expressed by SQBO (50 hPa level) and PV in the winter, known as the Holton-Tan effect (HT) (Holton and Tan, 1980). Labitzke & van Loon (1988) first found that the polar observations are significantly related to the solar period when the observations are bedded with a phase of SQBO in the equatorial stratosphere. Furthermore, the evidence that SQBO is also modulated with the solar cycle given by Salby and Callaghan (2000) due to the increased heat in the upper tropical stratosphere. The SQBO has been widely believed that it is generated mainly by Kelvin, Rossby-gravity, and gravity waves (Holton and Lindzen, 1972; Dunkerton, 1997).

SQBO affects not only the lower atmosphere but also the thermosphere and ionosphere, including the equatorial ionization anomaly (EIA: Equatorial Ionization Anomaly). EIA is found to be modulated by the phase of the SQBO. Chen (1992) provided evidence of the ionosphere response to SQBO and suggested that the day-to-day variability of EIA increases (decreases) with the eastern (western) phase of the SQBO at 40-50 hPa levels. This is mainly due to the change in an electric field through wave-tide interaction and then to the intensity change of Equatorial Electrojet, as suggested by Vineeth et al. (2011). The machine of neutral-wind dynamo effect (equatorial plasma fountain) seems to be the main cause of the ionosphere QBO, although the existence of a relationship between the solar and geomagnetic activities can not be removed (Neumann, 1990; Chen, 1992; Labitzke, 2005; Echer, 2007; Lu et al., 2009). Apostolov (1985), Chanin et al. (1989), and Kane (2005) provided the QBO variation to be determined by several solar and geomagnetic parameters. The signals of the QBO on the F2 layer of the ionosphere have also been demonstrated from the different latitude/longitude regions (Echer, 2007). The author proposed three possible mechanisms which could cause the ionosphere QBO: The first, the QBO in solar activity indices could compose the QBO signature in the ionosphere; The second, the QBO in the stratosphere influences the propagation of atmospheric waves which propagate upwards into F region of the ionosphere and affects the ionization and neutral wind circulation; The third, the ionosphere QBO could be generated from the QBO in geomagnetic activity and the Interplanetary Magnetic Field which influences the particle precipitation and the ionosphere current systems. The ionosphere QBO only occurs during solar maximum and exists in all latitudes from 50°S to 50°N (Tang et al., 2014). The author also shows that the ionosphere QBO expresses a significant characteristic of EIA, where the transition of phases appears 2-6 months later than in high latitudes. As we know, the structure of the low-latitude ionosphere is mainly controlled by the electrodynamics process, which produces EIA. Therefore, any change in electrodynamic characteristics will affect plasma distribution over equatorial and low-latitude regions. The ionosphere Total Electron Content (TEC) and wind data in the stratosphere show that the equatorial ionosphere responds distinctly different in the different QBO periods (Yadav et al., 2019). Using global TEC maps, Sun et al. (2022) showed that the QBO in global TEC at 40°S to 40°N latitudes and characterized by EIA. The author proposed that the mesosphere QBO is connected to the ionosphere QBO through the equatorial ionosphere fountain effect and neutral winds, which modulate the E region dynamo.

This paper studies the ionospheric QBO signal using continuous GPS data in Vietnam and the adjacent region (Southeast Asian region) for the period 2008-2021, more than 1 solar cycle. While the origin of QBO is disputed, we hope our results could contribute to a better understanding of it. The paper is organized into 4 sections. The first section describes SQBO, and its influence on other factors. The second section introduces the data and calculation methods. The third section delineates our work results and discussion. Then some conclusions are given in the fourth section.

2. Data and calculation method

The temporal-latitudinal TEC maps are established using the continuous GNSS data in the Southeast Asian region. The geographical coordinates and magnetic latitudes of the GNSS stations are listed in Table 1 and presented in Fig. 1. The data of some stations of the International GNSS Services (IGS): CMUM, CUSV, and CPNM in Thailand, ANMG in Malaysia, NTUS in Singapore, BAKO and JOG2 in Indonesia and XMIS in Australia are also used. The position of the magnetic equator in 2010 in the latitude of 7-8°N is also presented in Fig. 1.

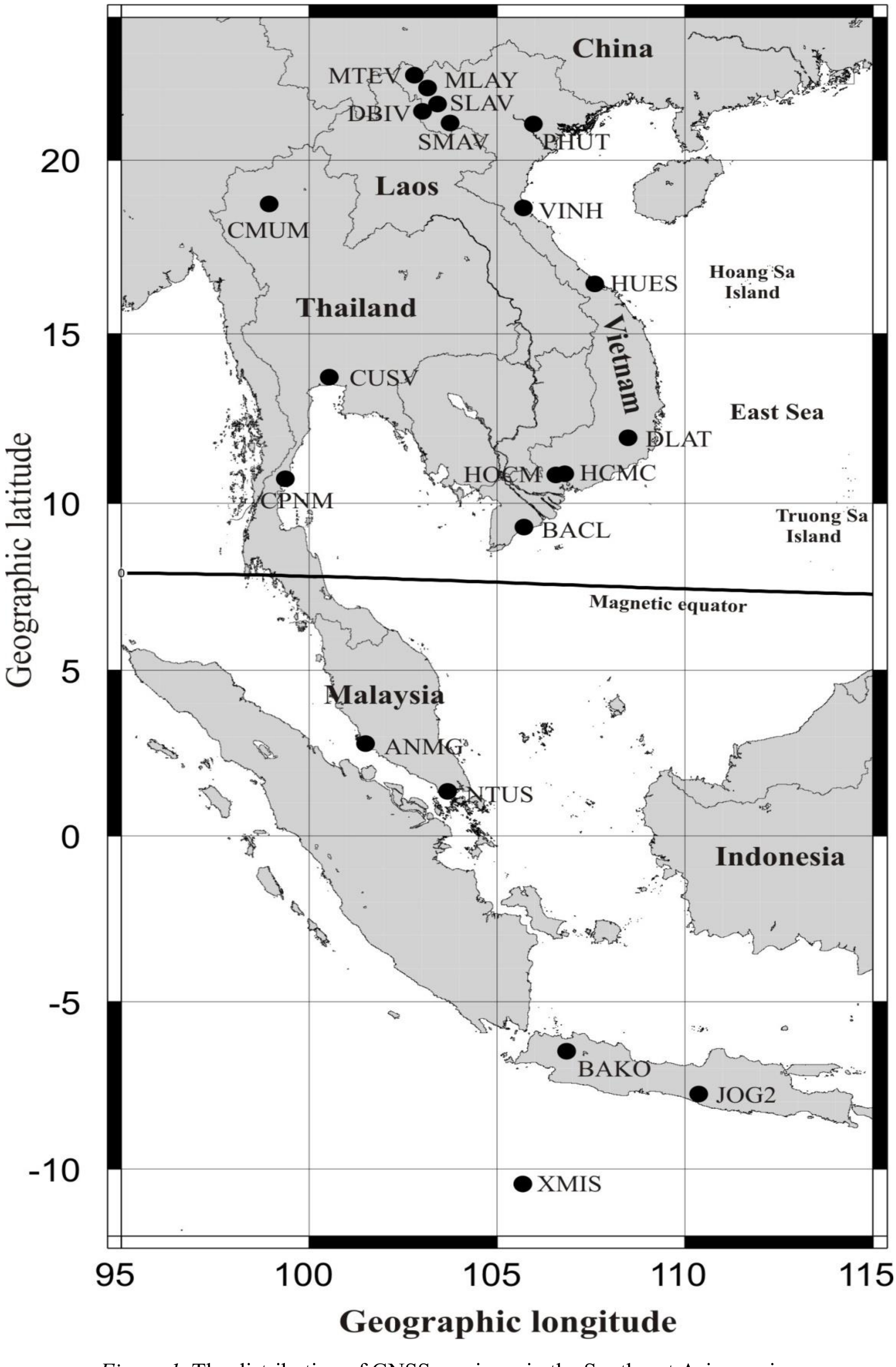

Figure 1. The distribution of GNSS receivers in the Southeast Asian region

Table 1. GNSS stations in the Southeast Asian region

No	Station	Geographical coordinate		Magnetic latitude	Instrument	Observation period
		Longitude	Latitude			
1	MTEV	102.80719	22.38719	15.92	NETRS	12/2009-12/2018
2	MLAY	103.15385	22.04187	15.54	NETRS	1/2012-12/2018
3	DBIV	103.01829	21.38992	14.84	NETRS	11/2009-12/2018
4	TGIV	103.41803	21.59225	15.06	NETRS	11/2009-12/2018
5	SMAV	103.74971	21.05629	14.49	NETRS	6/2010-7/2018
6	SLAV	103.90664	21.32529	15.19	NETRS	12/2009-09/2014
7	PHUT	105.95872	21.02938	14.49	GSV4004	2/2009-12/2021
8	VINH	105.69659	18.64999	11.91	CORS5700	9/2011-12/2021
9	HUES	107.59265	16.45919	9.58	GSV4004	1/2006-10/2011
10	DLAT	108.48175	11.94527	5.07	GSV4004	11/2014-12/2021
11	HOCM	106.55979	10.84857	3.47	GSV4004	01/2008-10/2012
12	HCMC	106.80139	10.87808	3.52	Net R9	2/2018-12/2021
13	BACL	105.75167	9.26806	2.73	GSV4004	05/2015-12/2021
14	CMUM	98.93238	18.76088	12.32	IGS station	01/2014-12/2021
15	CUSV	100.53392	13.73591	6.43	IGS station	5/2008-12/ 2021
16	ANMG	101.50660	2.78465	-5.14	IGS station	02/2014-12/2021
17	NTUS	103.67996	1.34580	-7.05	IGS station	1/2008-12/ 2021
18	BAKO	106.84891	-6.49106	-15.52	IGS station	1/2008-12/2021
19	JOG2	110.37272	-7.76377	-16.75	IGS station	10/2013-12/2021
20	XMIS	105.68350	-10.44996	-19.99	IGS station	01/2008-12/2021

The TEC values are calculated using the combination of the phase and pseudo-range measurements (Le Huy Minh et al., 2016b and reference therein). To evaluate the Quasi-Biennial Oscillation of two EIA crests, we calculated the monthly mean TEC amplitude of the EIA Northern and Southern crests. Le Huy et al. (2014) showed a very high correlation level between the monthly mean amplitude of the TEC at two crests and the sunspot number (~0.88). TEC amplitude variations share the same period features as solar activities. This paper introduces the monthly mean solar flux at 10.7 cm as the solar index. So to eliminate the impact of solar activities, we modeled the 11-year solar cycle as a second-order polynomial and 6- and 12-month periods as sinusoid and obtained the regression equation (Tang et al., 2014):

$$I_C^{(N,S)f} = A_0 + A_1F_{10.7}(t) + A_2F_{1.7}^2(t) + \left(B_0 + B_1F_{10.7}(t)\right)\sin\left(\frac{2\pi t}{T_1} + \theta_1\right) + \left(C_0 + C_1F_{10.7}(t)\right)\sin\left(\frac{2\pi t}{T_2} + \theta_2\right) \quad (1)$$

where T_1 and T_2 represent the seasonal variation with 6-month and 12-month periods, respectively; θ_1 and θ_2 represent the phases of the annual oscillation and semiannual oscillation, respectively; A_i, B_i, and C_i are regression coefficients which are calculated by the least square method. With the calculated regression coefficients and known monthly mean F10.7, we can obtain $I_C^{(N,S)f}$ curves that were fitted with $I_C^{(N,S)}$ observed values. The ionospheric QBO signal will be obtained from the residuals between the observed $I_C^{(N,S)}$ and the fitted $I_C^{(N,S)f}$.

3. The results and discussion

3.1. The equatorial ionization anomaly over the Southeast Asian region

The temporal-latitudinal VTEC maps (or TEC maps) were established by the method introduced in previous articles (Le Huy Minh et al., 2006; Le Huy et al., 2014, 2016a, 2016b) as well as in international publications (Huang et al., 1989; Liu et al., 1996; Tsai et al., 2001). Fig. 2 and Fig. 3 illustrate temporal-latitudinal monthly average TEC maps for 12 months in 2009 and

2014 over the Southeast Asian region, respectively, where 1 TECU = 10^{16}el/m^2. The contour maps in these two figures show month-to-month variations in the amplitude and locations of the EIA crests. The EIA crest can be characterized by occurrence time, latitude, and amplitude parameters. Still, in this paper, we only consider the amplitude parameter of the EIA crest; the time variation of the EIA crest on the occurrence time and the latitude parameters we will consider in the subsequent studies.

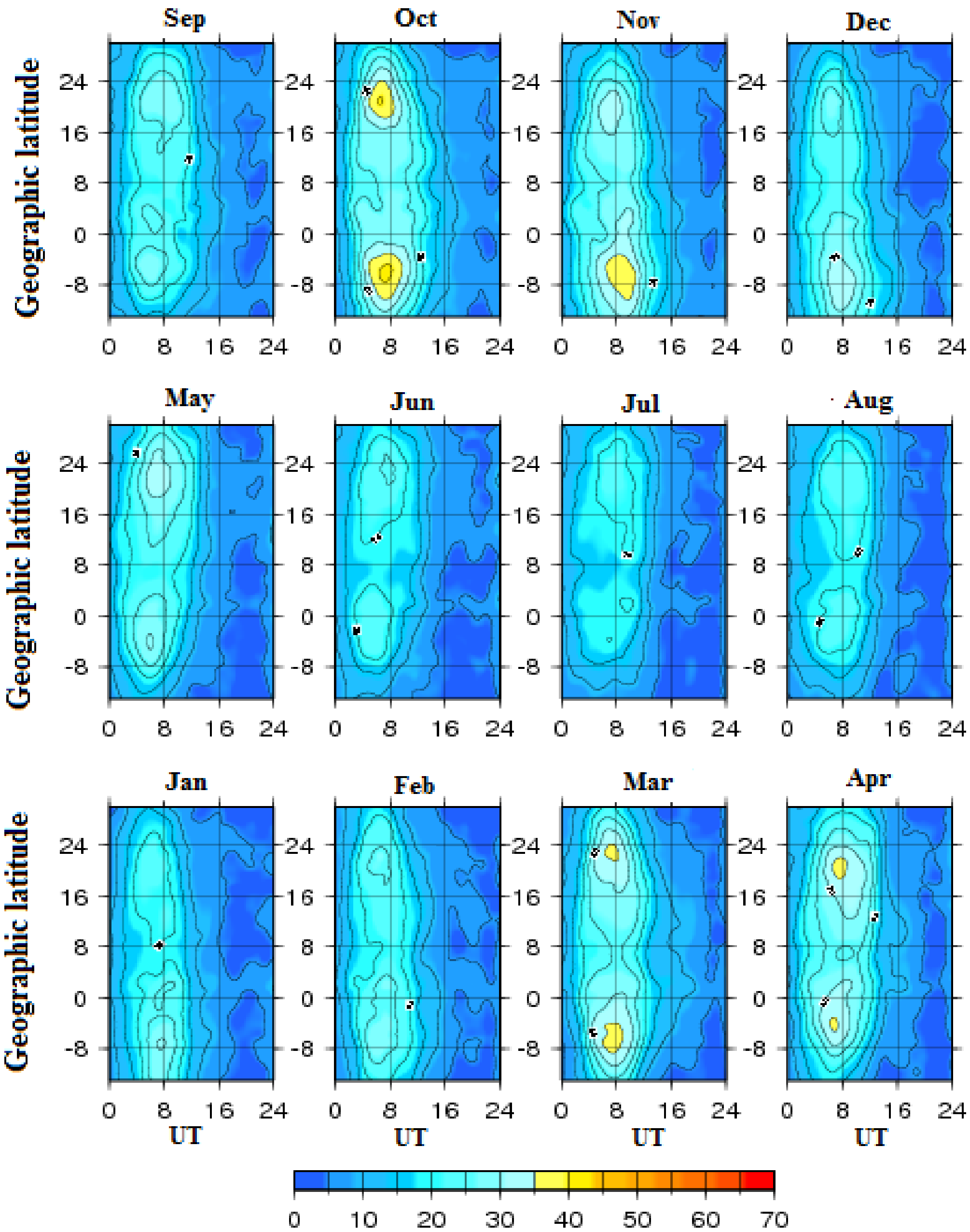

Figure 2. The temporal-latitudinal monthly average TEC maps in 2009. Contour interval of 5 TECU

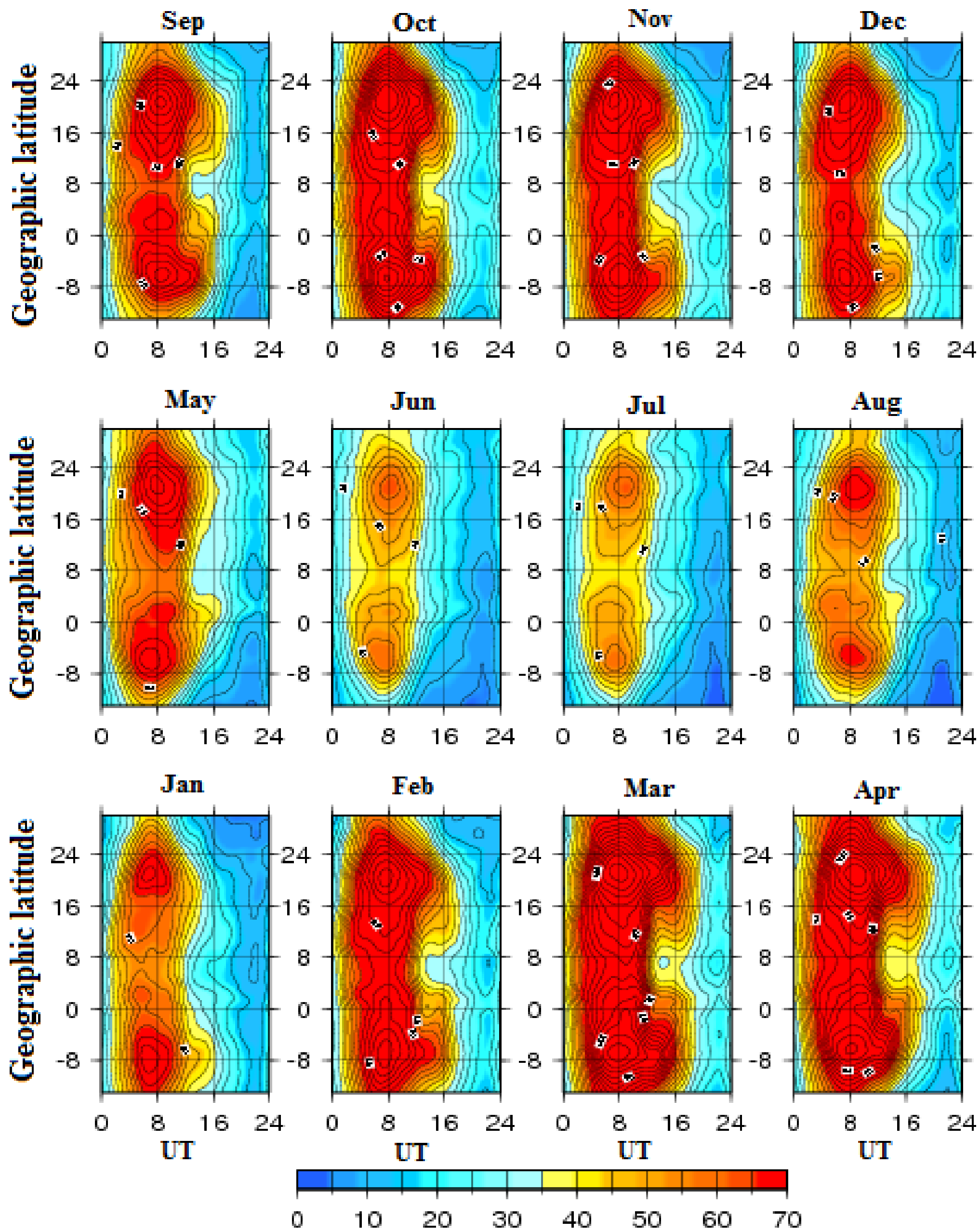

*Figure 3.*The temporal-latitudinal monthly average TEC maps in 2014. Contour interval of 5 TECU

Although the geomagnetic activity could affect the results, the normal days are dominant in a month. Therefore, the result of TEC maps is still clear and could be employed to reveal the ionosphere's normal behaviors. The months were marked from January to December from bottom to top and left to right. The horizontal axis is time UT (LT=UT+7), and the vertical axis is geographical latitude with a contour interval of 5 TECU. Magnetic equatorial is about 7-8°N geographic latitude on the IGRF2010 model. These maps are drawn in the same color scale to quickly compare the variation of monthly average TEC values from month to month and year to year.

Fig. 2 and Fig. 3 show that the monthly mean VTEC amplitude has two maximum peaks on two sides of the magnetic equator. The northern crest is observed near the latitude of 20°-22°N, i.e., in the Northern part of Vietnam, and the southern crest is observed in the latitude 5°-7°S. The TEC observed character was so-called the Equatorial Ionization Anomaly (EIA) of the ionosphere. TEC values are maximum in the time about from 05:00-09:00UT (12:00-16:00LT) and at the spring equinox (3, 4) and autumn equinox (9, 10). Its minimum values are in the summer months (5, 6, 7, 8) in the Northern Hemisphere and in the winter months (5, 6, 7, 8) in the Southern Hemisphere. In addition, TEC values are larger during the high solar activity period (2014) than those during the low solar activity period (2009). These results agree with Le Huy Minh et al. (2014, 2016a).

3.2. The ionosphere QBO at two EIA crests and the SQBO

Figs. 4a, b, c illustrate the monthly mean solar flux at 10.7 cm (F10.7) and the monthly mean amplitudes of crests (observed and fitted) from 2008 to 2021 at the northern and southern crests, respectively. The fitted curves are quite suitable for the observed, fully reflected solar activity, 1-year, and 6-months period variations. The crests' amplitude values depend on the solar activity; they have low values during the years of low solar activity (2008, 2009, 2018, 2019). In 2010, they increased when the Sun entered the ascending phase of the solar sunspot cycle 24. During the years of solar sunspot maximum (2011, 2012, 2013, 2014), they have large values. In 2020, the Sun entered the ascending phase of the solar sunspot cycle 25, the crests' amplitude values had an increasing trend. It reaches a maximum value of about 120 TECU and a minimum of about 20 TECU. The variation trend of EIA crests, in general, is suitable for solar activity. Fig. 4b and Fig. 4c also show that the EIA crests have semiannual and annual variation trends. Solar activity is reasonably the main factor affecting the 11 years, annual and semiannual oscillations of the amplitude of crest of TEC.

First we calculated the difference between the observed $I_C^{(N,S)}$ and fitted $I_C^{(N,S)f}$ values to obtain the quasi-biennial oscillation signals in EIA crests amplitudes. The obtained residuals, ΔTEC, are presented in Figs. 5a and 5b for northern and southern crests, respectively. The maximum amplitudes of the residuals are -23 TECU and -15 TECU for northern and southern crests, respectively, which are about 20% and 13% of the maximum values.

To find the QBO signals in the EIA crests amplitudes, the ΔTEC residuals have been analyzed by the Lomb-Scargle periodogram methods (Lomb, 1976, Scargle, 1982). Figure 6 illustrates the Lomb-Scargle spectrum with a period from 1 to 36 months of ΔTEC at the northern crest (red line) and the southern crest (blue line). Some spectrum peaks within the periods related to the stratosphere QBO: 18, 25, and 29-30 months, responsible for the QBO-like signal. The signal shares a similar period with the SQBO. The spectrum amplitude of 18 months period is 3.8 and 4.6 TECU for northern and southern crests, respectively; about 16.5% and 30% of the maximum residuals ΔTEC, which are greater than the one obtained by Tang et al. (2014) (about 10%). Because the semiannual and annual variations of EIA crests are eliminated by the fitting method, so the spectrum peaks of the periods of 6 and 12 months are absent. But some periods of 4, 8, and 10 months exist in the residuals, which will be analyzed in other studies. The spectrum in Fig. 6 illustrates that the possible effect of SQBO is included in the EIA crests amplitude, the residual variations will be analyzed in the following.

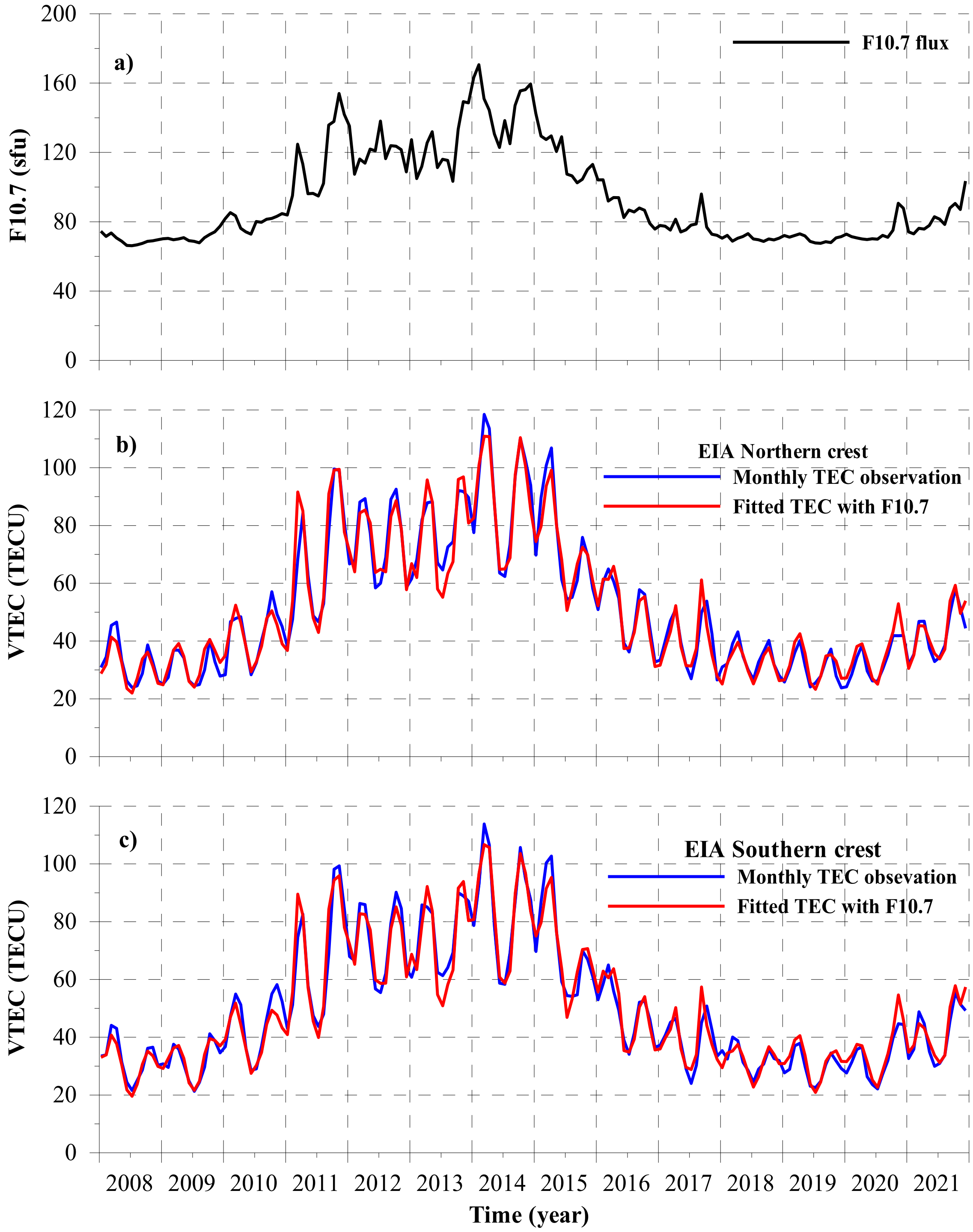

Figure 4. a) Monthly mean solar flux at F10.7 cm; Monthly mean TEC amplitude variation (blue line) at two EIA crests and TEC values were fitted by a polynomial with parameter F10.7 (red line) in the period from 2008 to 2021 for b) northern crest, c) southern crest

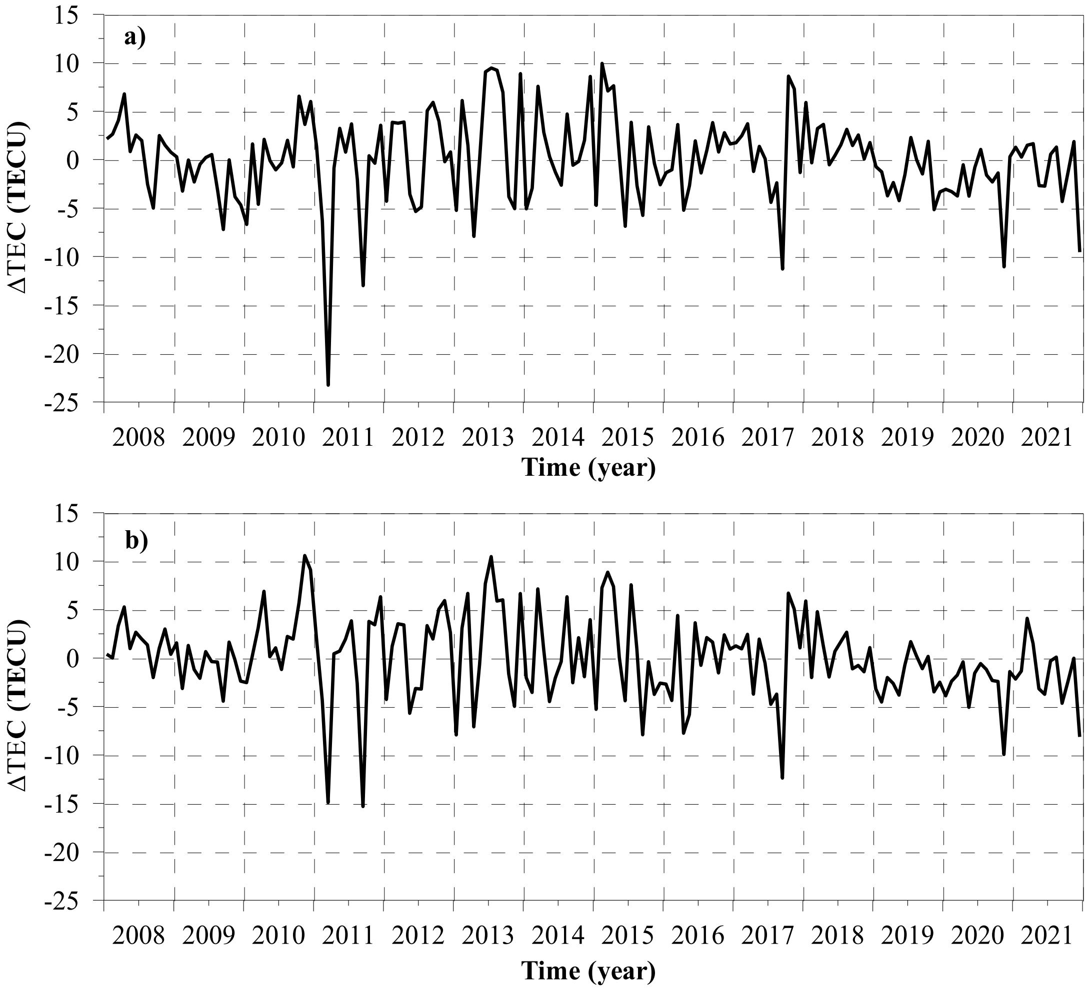

Figure 5. The variation of ΔTEC residuals after subtracting the amplitudes fitted with F10.7 from monthly mean EIA crests amplitudes for the period 2008-2021 a) for the northern crest, b) for the southern crest

So, to obtain the QBO signal in the EIA crests amplitudes, we used a band-pass filter centered at 25 months with haft-power points at 17 and 33 months for the ΔTEC residuals. The obtained ionospheric QBO and the SQBO which is the zonally averaged winds from the CDAS Reanalysis data at 50 hPa (~20 km) (http://www.cpc.ncep.noaa.gov/data/indices/), are presented in Fig. 7. This figure indicates that during low solar activity in 2008-2009, the ionospheric QBO signal was unclear. This result is somewhat consistent with Tang et al. 2014. From 2010 to 2021, the ionospheric QBO signals at the two EIA crests are very clear.

Comparing the SQBO and the obtained ionospheric QBO, we can see that their relationship is quite complicated. For the 2008-2009 period, the ionospheric QBO is not clear, as mentioned above; SQBO and ionosphere QBO signals are in phase for the 2010-2013 and 2018-2021 periods but anti-phase for 2014-2017. Their correlation coefficients in three periods are 0.623, 0.637, and -0,646 for the EIA northern crest and 0.571, 0.538, and -0.530 for the southern crest, respectively. The correlation between SQBO and EIA crests QBO in the northern crest is higher than in the southern one.

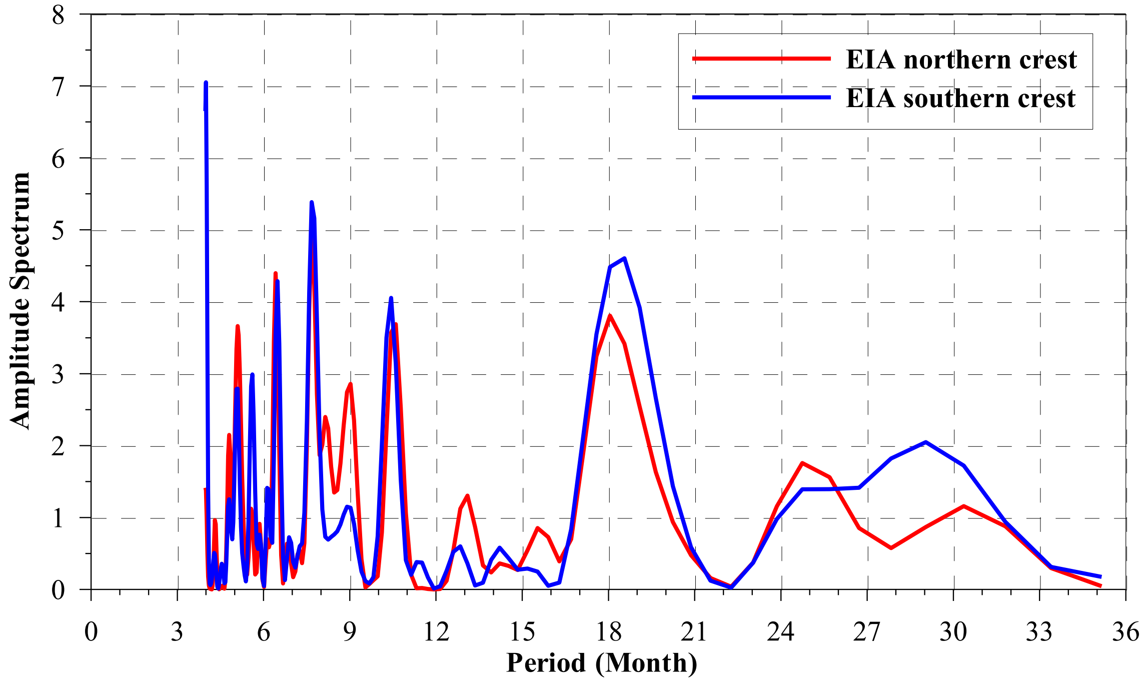

Figure 6. Lomb-Scargle periodogram for the ΔTEC variations at two EIA crests are presented in red line for the northern crest and in blue line for the southern crest

Figure 7 also shows that during the period 2015-2016, the stratospheric QBO signal shortened, its period is ~1.5 years. We also observe a shortening of the QBO cycle at the two EIA crests. During the period 2015-2016 of the ENSO (El-Niño - Southern Oscillation) warm phase, ENSO controlled stratospheric QBO, and in the strong warm phase of ENSO, SQBO had a shortened period of ~1.5 years (Sun et al., 2018). During this period, the correlation coefficient between SQBO and ionosphere QBO are -0.631, and -0.521 for the northern and southern crests, respectively, as mentioned above. In comparison between the band-filtered TEC observations (ionospheric QBO) at the geomagnetic latitude of 15°N, 0°, 15°S at 18LT and the zonally averaged winds as an indicator of the SQBO for the 1999-2011 period, Tang et al. (2014) showed that the ionospheric QBO exist from 1999 to 2005 and two years after 2009. During this period, the ionospheric QBO exhibits a positive correlation with the SQBO, and the correlation coefficients reach 0.704. The authors considered that the ionospheric QBO is not found in the TEC observations during solar minimum. Figure 7 shows that in minimum solar periods 2008-2009 and 2019-2020, the ionospheric QBO amplitudes are different, low in the 2008-2009 period but significant in the 2019-2020 period. So, we cannot generally conclude that the minimum ionospheric QBO is low during solar.

We used the cross wavelet transform to evaluate common variation between SQBO and Ionosphere QBO at two EIA crests

(Grinsted et al., 2004). Fig. 8 and Fig. 9 show the results of the cross wavelet transform from the software package Torrence and Compo (1998) of SQBO and the obtained ionospheric QBO signals. Color representation in Fig. 8 and Fig. 9 indicates the wavelet power. The red bands indicate high wavelet power corresponding to 16-34 months, which are ionosphere QBO and SQBO. From 2010 through 2013, at two EIA crests, cross wavelet transform presents the arrows tend to turn to the right, which proves that in this period, the SQBO and ionosphere QBO are in phase. In 2014, the arrows have a gradual reversal, from the right-turning trend gradually leaning to the left side until the end of 2017, which shows the opposite phase relationship between the SQBO and the ionosphere QBO in the period 2014-2017. In the period from 2018 to 2021, the arrows point to the right, which proves that the relationship between the SQBO and the ionosphere QBO at the two EIA crest is in phase. The results of the cross wavelet transform between the SQBO and the ionosphere QBO at the two EIA crests are consistent with the results of the correlation analysis between them.

The results of our study are somewhat consistent with the results given by Tang et al., 2014, which could consider that the ionospheric QBO is affected by the SQBO. In addition, in 2015-2016, the SQBO and the QBO at the two EIA crests were shortened. Sun et al. (2018) concluded that the 2015-2016 period is in the warm phase of ENSO in which the ENSO can modulate the SQBO. Fig. 6 of Tang et al. (2014) showed that during the 2006-2007 period, the SQBO signal was shortened, its period was about 1.5 years, and the amplitude of ionospheric QBO was low anti-phase with the SQBO. 2006-2007 was also in the warm phase of ENSO (McPhaden, 2008). The similarity of the ionospheric QBO signals for the periods 2006-2007 and 2015-2016 may indicate that during the warm phase of ENSO, the period of the atmospheric QBO is shortened, the period of the ionospheric QBO is also shortened, the magnitude is reduced and out of phase with the atmospheric QBO. In addition, knowing that the period from July 2009 to April 2010 is in the warming phase of ENSO (https://psl.noaa.gov/enso/mei/), Fig. 7 also shows a decrease in the amplitude of ionosphere QBO. These observations may allow us to have a more basic to conclude that the SQBO is the important factor affecting the ionospheric QBO at two EIA crests.

It is well-known that SQBO is a downward propagation of alternating westerly and easterly zonal wind shears in the tropical stratosphere with a period of ~28 months. It is driven mainly by equatorially trapped gravity waves propagating from the troposphere to the stratosphere. Diallo et al. (2017) discussed the mechanism of 2015/16 disrupted QBO and showed that during the winter of 2015/16, an unexpected shift from westerly (w_{QBO}) to easterly (e_{QBO}) winds occurred. In January 2016, e_{QBO} phase developed in the center of the w_{QBO} phase early before the w_{QBO} phase completed the 28 months cycle. Planetary Rossby waves propagating from the Northern Hemisphere to the Southern Hemisphere in the winter stratosphere mostly accounted for the QBO disruption (Osprey et al., 2016). During the winter, planetary waves usually propagate upward from mid-latitudes to the upper stratosphere, break and deposit their westward momentum there. In February 2016, a strong easterly subtropical jet developed in the upper stratosphere between 35-10 hPa, which prevented the waves from propagating upward, causing them to be reflected horizontally equatorward. The austral summertime westward winds prevented the Rossby waves from propagating into the southern hemisphere, resulting in wave breaking and westward acceleration. These changes in the stratosphere likely influence the ionosphere (Wang et al., 2017).

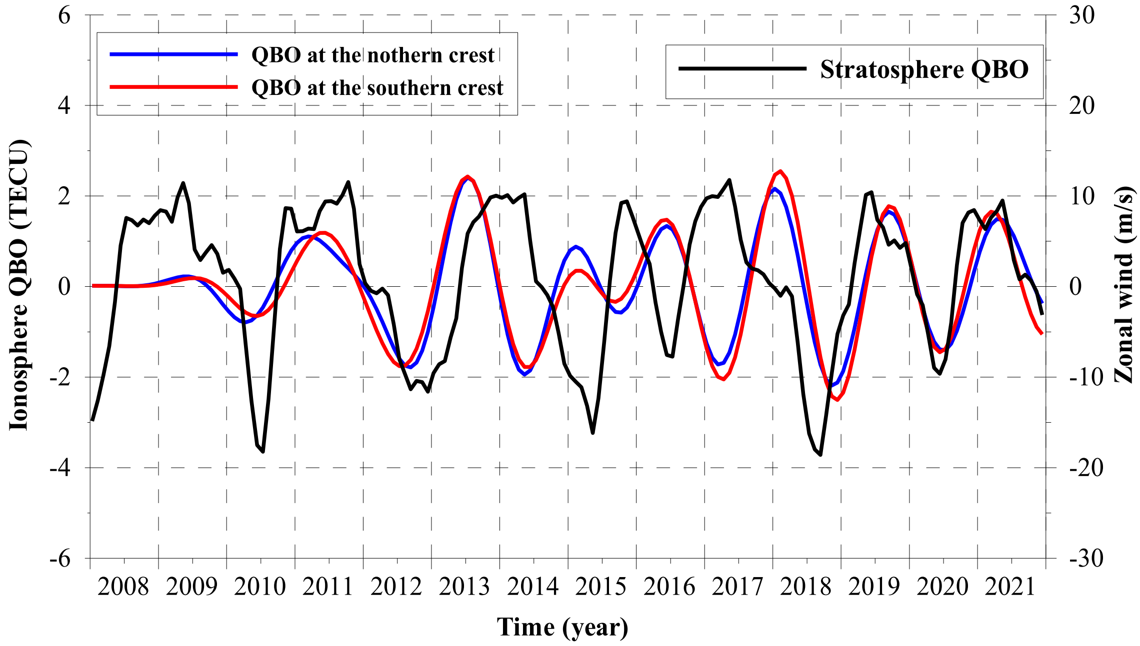

Figure 7. Comparison of the ΔTEC values filtered by band-pass filter and stratospheric QBO at 50 hPa. The filtered components at the northern and southern crests are plotted with red and blue lines, respectively. The black line shows the stratospheric QBO at 50 hPa

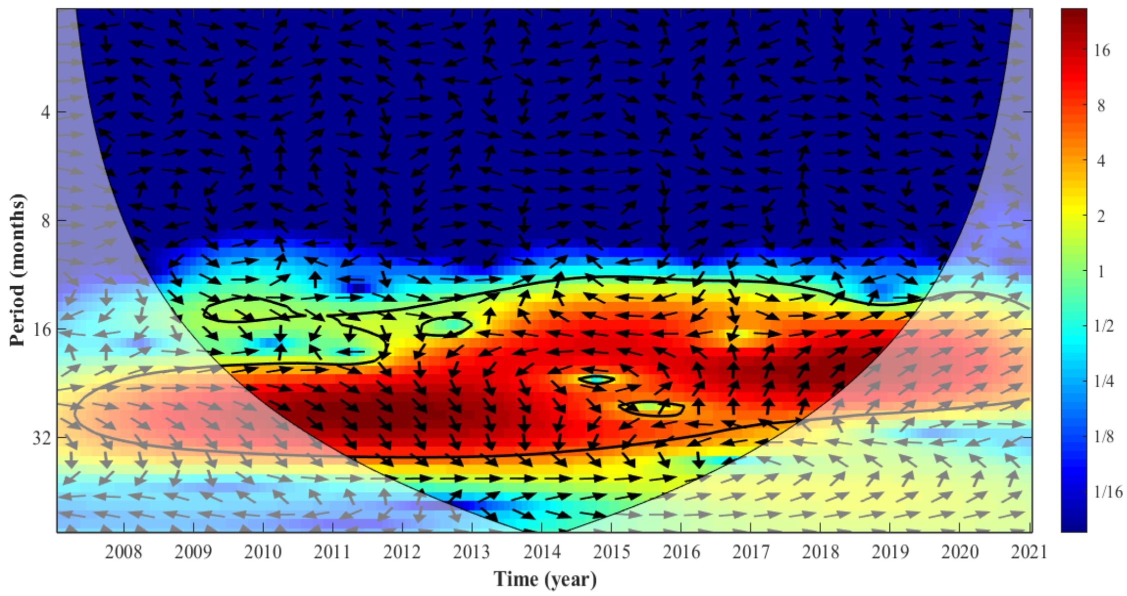

Figure 8. Cross-wavelet transform of the ionosphere QBO of the northern crest and the SQBO. The 95% confidence is shown as a thick contour; the cone of influence (COI), where edge effects might distort the picture, is shown as a lighter shade. The relative relationship is shown as arrows (with in-phase pointing right, anti-phase pointing left)

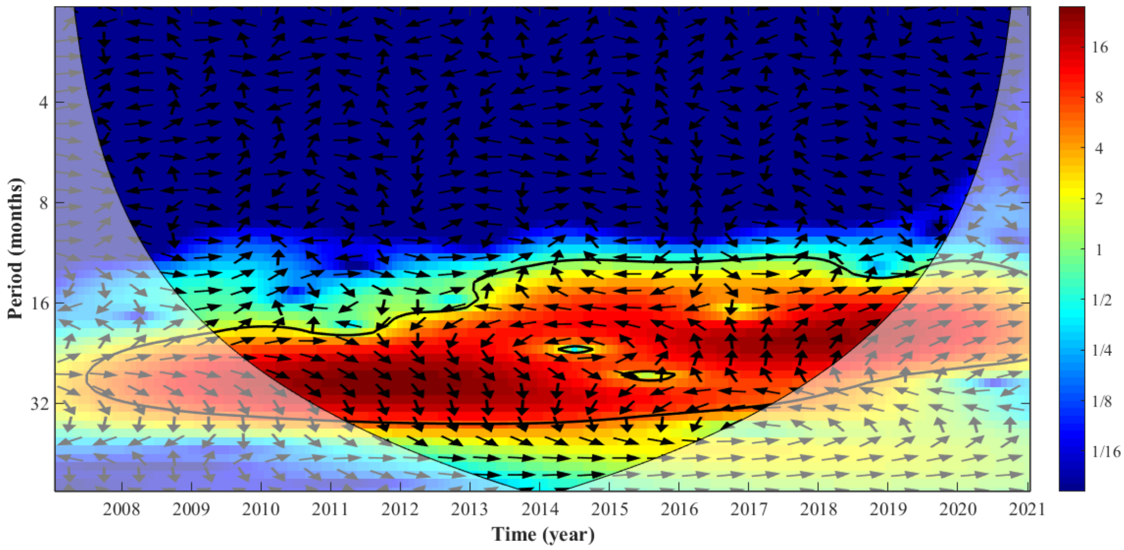

Figure 9. The same as Fig. 8 for the southern crest

The quasi-biennial oscillations of the solar irradiance flux have been considered the major contributor to the quasi-biennial oscillations in the ionosphere (Fernández et al., 2014). QBO is not only strongly present in the solar irradiance proxy during a period of high solar activity but also in low-latitude electron content values during the same period but is weakly expressed at the magnetic equator (Dashora and Suresh, 2015). The results of this study show that QBO in solar radiation proxy is expressed in low-latitude ionospheric QBO with latitude dependence. It is reinforced by the fact that during solar minimum, the power in the QBO scales of the electron content decreases. Therefore, the role of stratospheric QBO in inducing low-latitude ionospheric QBO variation is unclear. The existence of an ionospheric QBO is still an open question due to different theories on its origin (Echer, 2007), which are partly influenced by the stratospheric QBO (Tang et al., 2014; Mansilla et al., 2009) and by the solar/geomagnetic QBO (Kane, 1995; Echer, 2007). However, in our study, the influence of solar activity on the variations of two EIA crests was eliminated. We assumed that other existing ionospheric - thermosphere coupling mechanisms contribute to the variation of two EIA crests. In addition, given the geomagnetic origin of QBO, we believe it refers to interplanetary activity and its impact on variations in the geomagnetic field (Dashora and Suresh, 2014).

Furthermore, the variations in the geomagnetic field due to ionospheric dynamics as studied by Yacob and Bhargava (1968), Sugiura and Poros (1977), and Olsen and Kiefer (1995) were not related to the proposed variations by Kane (1995) and Echer (2007). Up to now, the origin of ionospheric QBO is thought to be due to some factors such as solar activity, geomagnetic activity, and atmospheric QBO. As mentioned above, our results show that the stratospheric QBO is the main factor affecting the ionospheric QBO at two EIA crests. However, the physical theoretical interpretation of these mechanisms of action is still a challenge for scientists and requires further research.

4. Conclusions

In this paper, we have studied the biennial oscillation characteristic of the equatorial ionization anomaly peak using TEC data obtained from the continuous GPS network over Vietnam and the adjacent region during the period 2008-2021; the following is a summary of the new findings of this study.

The EIA crests exist at 20-22°N and about 5-6°S on either side of the magnetic equator. The maximum TEC value is during 05:00-09:00UT (12:00-16:00LT). The amplitude of the EIA crests is greatest during the spring equinox (3, 4) and autumn equinox (9, 10). It has the smallest value in the summer period (5, 6, 7, 8) in the Northern Hemisphere and in the winter period (5, 6, 7, 8) in the Southern Hemisphere.

The observed QBO signal is present at two EIA crests. Its period is 18 months to 34 months which has the same period as the stratospheric QBO. During low solar activity from 2008 to 2009, the QBO-like signal is low. In 2019-2020, we observed a clear QBO signal.

The correlation coefficient between stratospheric QBO and ionospheric QBO at two EIA crests in 2010-2013, 2014-2017, and 2018-2021periods are 0.623, -0.646, 0.637 for the Northern Hemisphere, and 0.571, -0.530, 0.538 for the Southern Hemisphere, respectively.

During 2015-2016, the warm phase of ENSO, the stratospheric QBO, was shortened; its period is ~1.5 years. We also observed a shortening of the ionospheric QBO period at the two EIA crests. The correlation coefficient between the period of the stratospheric QBO and the ionosphere QBO is -0.631 for the northern crest and -0.521 for the southern crest.

The results of the cross-wavelet transform between the stratospheric QBO and the ionospheric QBO at the two EIA crests also show that they are in phase in the 2010-2013 and 2018-2021 periods but anti-phase in the 2014-2017 period.

The results in this study provide exciting features of the QBO feature at the EIA crest over Vietnam and the adjacent region, contributing essential information for building regional and global ionospheric models.

Acknowledgments

We are thankful to the anonymous referees for reviewing and helping us to improve our paper and to the IGS Community for making available GNSS data. This study has been supported by the Vietnam Academy of Science and Technology under the CSCL12.01/22-22 and NVCC 12.02/22-22 grant numbers.

References

Apostolov E.M., 1985. Quasi-biennial oscillation in sunspot activity, Bull. Astron., 36, 97-102.

Baldwin M.P., L.J. Gray, T.J. Dunkerton, K. Hamilton, P.H. Haynes, W.J. Randel, J.R. Holton, M.J. Alexander, I. Hirota, T. Horinouchi, D.B.A. Jones, J.S. Kinnersley, C. Marquardt, K. Sato, M. Takahashi, 2001. The quasi-biennial oscillation, Rev. Geophys., 39, 179- 229.

Burrage M.D., R.A. Vincent, H.G. Mayr, W.R. Skinner, N.F. Arnold, P.B. Hays, 1996. Long-term variability in the equatorial middle atmosphere zonal wind, J. Geophys. Res., 101, 12847-12854. Doi: 10.1029/96jD00575.

Chanin M.L., P. Keckhut, A. Hauchecorne, K. Labitzke, 1989. The solar activity-QBO, effect in the lower thermosphere, Ann. Geophys., 32, 225-230.

Chen P., 1992. Evidence of the ionospheric response to the QBO, Geophys. Res. Lett., 19, 1089-1092.

Dashora N., S. Suresh, 2015. Characteristics of low-latitude TEC during solar cycles 23 and 24 using global ionospheric maps (GIMs) over Indian sector, J. Geophys. Res. Space Phys., 120(6), 5176-5193. Doi: 10.1002/2014ja020559.

Diallo M., C. Schwartz, A. Kebede, 2017. Response of stratosphere tracers to the 2015/2016 QBO disruption, Conference: Training school on stratosphere-troposphere interactions, 2-5 September 2017 at University of Cape Town, South Africa.

Dunkerton T., 1997. The role of gravity waves in the quasi-biennial oscillation, J. Geophys. Res., 102(D22), 26053-26076.

Ebdon R.A., R.G. Veryard, 1961. Fluctuations in equatorial stratospheric winds, Nature, 189, 791-793.

Echer E., 2007. On the quasi- biennial oscillation (QBO) signal in the foF2 ionospheric parameter, J. Atmos. Sol. Terr. Phys., 69, 621-627.

Espy P.J., S.O. Fernández, P. Forkman, D. Murtagh, J. Stegman, 2011. The role of the QBO in the inter-hemispheric coupling of summer mesospheric temperatures, Atmos. Chem. Phys., 11, 495-502. Doi: 10.5194/acp-11-495-2011.

Fernández L.I., A.M. Meza, A.G. Elías, 2014. Quasi-biennial oscillation in GPS VTEC measurements, Adv. Space Res., 54(2), 161-167. Doi: 10.1016/j.asr.2014.03.027.

Ford E.A.K., R.E. Hibbins, M.J. Jarvis, 2009. QBO effects on Antarctic mesospheric winds and polar vortex dynamics, Geophys. Res. Lett., 36, L20801. Doi: 10.1029/2009GL039848.

Grinsted A., J.C. Moore, S. Jevrejeva, 2004. Application of the cross wavelet transform and wavelet coherence to geophysical time series, Nonlinear Processes Geophys., 11, 561-566, SRef-ID: 1607-7946/npg/2004-11-561.

Hibbins R.E., M.J. Jarvis, E.A.K. Ford, 2009. Quasi-biennial oscillation influence on long-period planetary waves in the Antarctic upper mesosphere, J. Geophys. Res., 114, D09109. Doi: 10.1029/2008JD011174.

Holton J.R., R. S. Lindzen, 1972. An updated theory for the quasi-biennial cycle of the tropical stratosphere, J. Atmos. Sci., 29, 1076-1080.

Holton J.R., H.C. Tan, 1980. The influence of the equatorial quasi- biennial oscillation on the global circulation at 50 mb, J. Atmos. Sci., 37, 2200-2208. https://doi.org/10.1016/j.jastp.2009.04.002.

Huang Y.N., K. Cheng, S.W. Chen, 1989. On the equatorial anomaly of the ionosphere total electron content near the northern anomaly crest region. J. Geophys. Res., 94(A10), 13515-13525.

Kane R.P., 1995. Quasi-biennial oscillation in ionospheric parameters measured at Juliusruh (55°N, 13°E), J. Atmos. Terr. Phys., 57, 415-419.

Kane R.P., 2005. Differences in the quasi-biennial oscillation and quasi-triennial oscillation characteristics of the solar, interplanetary and terrestrial parameters. J. Geophys. Res.: Space Phys., 110, A01108.

Labitzke K., 1987. Sunspots, the QBO, and the stratospheric temperature in the north polar region, Geophys. Res. Lett., 14(5), 535-537. Doi: 10.1029/gl014i005p00535.

Labitzke K., 1982. On the Interannual Variability of the Middle Stratosphere during the Northern Winters. J. Meteorol. Soc. Japan, 60(1), 124-139.

Labitzke K., 2005. On the solar cycle-QBO relationship: a summary, J. Atmos. Sol.Terr. Phys., 67 (Special Issue), 45-54.

Labitzke K., H. van Loon, 1988. Association between the 11- year solar cycle, the QBO and the atmosphere, part I, The troposphere and stratosphere in the Northern Hemisphere in winter, J. Atmos. Terr. Phys., 50, 197-206.

Le Huy Minh, A. Bourdillon, P. Lasudrie Duchesne, R. Fleury, Nguyen Chien Thang, Tran Thi Lan, Ngo Van Quan, Le Truong Thanh, Hoang Thai Lan, Tran Ngoc Nam, 2006. Determination of the ionospheric total electron content in Vietnam using the data from three GPS receivers at Hanoi, Hue and Hoc Mon. J. Geology, A296, 53-62 (in Vietnamese).

Le Huy M., C. Amory-Mazaudier, R. Fleury, A. Bourdillon, P. Lassudrie-Duchesne, L. Tran Thi, T. Nguyen Chien, T. Nguyen Ha, P. Vila, 2014. Time variations of the total electron content in the Southeast Asian equatorial ionization anomaly for the period 2006-2011, Adv. Space Res., 54, 355-368. Doi: 10.1016/ j.asr.2013.08.03.

Le Huy Minh, Tran Thi Lan, C. Amory-Mazaudier, R. Fleury, A. Bourdillon, J. Hu, Vu Tuan Hung, Nguyen Chien Thang, Le Truong Thanh, Nguyen Ha Thanh, 2016a. Continuous GPS network in Vietnam and results of study on the total electron content in the South East Asian region. Vietnam Journal of Earth Sciences, 38(2) 153-165.

Le Huy Minh, Tran Thi Lan, R. Fleury, C. Amory Mazaudier, Le Truong Thanh, Nguyen Chien Thang, Nguyen Ha Thanh, 2016b. TEC variations and ionospheric disturbances during the magnetic storm in March 2015 observed from continuous GPS data in the Southeast Asia region. Vietnam Journal of

Earth Sciences, 38(3), 267-285.

Liu J.Y., H.F. Tsai, T.K. Jung, 1996. Total electon content obtained using the global positioning system, TAO, 7(1), 07-17.

Lomb N.R., 1976. Least-squares frequency analysis of unequally spaced data, Astrophys. Space Sci., 39, 447-462.

Lu H., D. Pancheva, P. Mukhtarov, I. Cnossen, 2012. QBO modulation of traveling planetary waves during northern winter, J. Geophys. Res., 117, D09104. Doi: 10.1029/2011JD016901.

Lu H., Gray L.J., Baldwin M.P., Jarvis M.J., 2009. Life cycle of the QBO-modulated 11-year solar cycle signals in the Northern Hemispheric winter, Quaterly J. Royal Meteorol. Soc., 135, 1030-1043.

Mansilla G.A., P. Fernandez de Campra, M. Zossi de Artigas, 2009. Quasi-biennial oscillation in foF2 at the south crest of the equatorial anomaly, J. Atmos. Sol. Terr. Phys., 71(14), 1610-1612.

McPhaden M.J., 2008. Evolution of the 2006-2007 El Niño: the role of intraseasonal to interannual time scale dynamic, Adv. Geosci., 14, 219-230.

Mohamakumar K., 2008. Stratosphere Troposphere Interaction, An introduction, Springer, 416p.

Murphy D.J., S.P. Alexander, R.A. Vincent, 2012. Interhemispheric dynamical coupling to the southern mesosphere and lower thermosphere, J. Geophys. Res., 117, D08114. Doi: 10.1029/2011JD016865.

Naujokat B., 1986. An Update of the Observed Quasi-Biennial Oscillation of the Stratospheric Winds over the Tropics, J. Atmos. Sci., 43(17), 1873-1877.

Neumann A., 1990. QBO and solar activity effects on temperatures in the mesopause region, J. Atmos. Terr. Phys., 52, 165-173.

Olsen N., M. Kiefer, 1995. Geomagnetic daily variations produced by a QBO in thermospheric prevailing winds, J. Atmos. Sol. Terr. Phys., 57(13), 1583-1589.

Osprey S.M., N. Butchart, J.R. Knight, A.A. Scaife, K. Hamilton, J.A. Anstey, V. Schenzinger, C. Zhang, 2016. An unexpected disruption of the atmospheric quasi-biennial oscillation. Science, 353(6306), 1424-1427.

Physical Sciences Laboratory. https://psl.noaa.gov/enso/mei/.

Reed R.J., W.J. Campbell, L.A. Rasmussen, D.G. Rogers, 1961. Evidence of a downward-propagating, annual wind reversal in the equatorial stratosphere, J. Geophys. Res., 66(3), 813-818. Doi: 10.1029/jz066i003p00813.

Salby M., P. Callaghan, 2000. Connection between the Solar Cycle and the QBO, J. Climate, 13(14), 2652-2662. Doi: 10.1175/1520-0442(1999).

Scargle J.D., 1982. Studies in astronomical time series analysis. II. Statistical aspects of spectral analysis of unevenly spaced data. Astrophys. J., 263, 835-853.

Sugiura M., D.J. Poros, 1977. Solar-generated quasi-biennial geomagnetic variation, J. Geophys. Res., 82, 5621-5628. Doi: 10.1029/JA082i035p05621.

Sun Y.Y., H. Liu, Y. Miyoshi, L. Liu, L.C. Chang, 2018. El Niño-Southern Oscillation effect on quasi-biennial oscillations of temperature diurnal tides in the mesosphere and lower thermosphere, Earth. Planets Space, 70-85. Doi: 10.1186/s40623-018-0832-6.

Sun R., S.-Y.Gu, X. Dou, R. Zhang, J. Kuai, T. Tsuda, 2022. The impact of the quasi-biennial oscillation on the mesosphere and ionosphere. J. Geophys. Res. Space Phys., 127, e2021JA029920. https:/doi.org/10.1029/2021JA029920.

Tang W., X.H. Xue, J. Lei, X.K. Dou, 2014. Ionospheric quasi-biennial oscillation in global TEC observations, J. Atmos. Solar-Terr. Phys., 107, 36-41.

Torrence C., G.P. Compo, 1998. A practical guide to wavelet analysis, Bull. Am. Meteorol. Soc., 79, 61-78.

Tsai H.F., J.Y. Liu, W.H. Tsai, C.H. Liu, 2001. Seasonal variations of the ionpsheric total electron content in Asian equatorial anomaly regions, J. Geophys. Res., 106(A12), 30363-30369.

Venkat Ratnam M., G.K. Kumar, B.V.K. Murthy, A.K. Patra, V.V.M.J. Rao, S.V.B. Rao, K.K. Kumar, G. Ramkumar, 2008. Long-term variability of the low latitude mesospheric SAO and QBO and their relation with stratospheric QBO, Geophys. Res. Lett., 35, L21809. Doi: 10.1029/2008GL035390.

Vineeth C., T.K. Pant, K.K. Kumar, S.G. Sumod, S. Gurubaran, R. Sridharan, 2011. Planetary wave tidal interactions over the equatorial mesosphere-lower thermosphere region and their possible implications for the equatorial electrojet, J. Geophys. Res., 116, A01314. Doi: 10.1029/2010JA015895.

Wallace J.M., V.E. Kousky, 1968. Observational evidence of Kelvin waves in the tropical stratosphere, J. Atmos. Sci., 25, 900-907.

Wallace J.M., 1973. General circulation of the tropical lower stratosphere, Rev. Geophys. Space Phys., 11(2), 191-222. Doi: 10.1029/rg011i002p00191.

Wang J.C., R. Tsai-Lin, L.C. Chang, Q. Wu, C.C.H. Lin, J. Yue, 2017. Modeling study of the ionosphere responses to the quasi-biennial oscillations of the sun and stratosphere, J. Atmos. Sol.-Terr. Phys., 171, 119-130. Doi: 10.1016/j.jastp.2017.07.024.

Xu J., A.K. Smith, H.-L. Liu, W. Yuan, Q. Wu, G. Jiang, M.G. Mlynczak, J.M. Russell III, S.J. Franke, 2009. Seasonal and quasi-biennial variations in the migrating diurnal tide observed by Thermosphere, Ionosphere, Mesosphere, Energetics and Dynamics (TIMED), J. Geophys. Res., 114, D13107. Doi: 10.1029/2008JD011298.

Yacob A., B.N. Bhargava, 1968. On 26-month periodicity in quiet-day range of geomagnetic horizontal force and in sunspot number. J. Atmos. Terr. Phys., 30(11), 1907-1911.

Yadav S., C. Vineeth, K. K. Kumar, R. K. Choudhary, T.K. Pant, S. Sunda, 2019. The role of the phase of QBO in modulating the influence of the SSW effect on the Equatorial Ionosphere. J. Geophys. Res: Space Physics, 124. Doi: 10.1029/2019JA026518.